



Loma Linda University Electronic Theses, Dissertations & Projects

6-1976

Computer Assisted Electron Spin Resonance Spectral Analysis of Trapped Radicals

Philip Mook Wah Law

Follow this and additional works at: <https://scholarsrepository.llu.edu/etd>



Part of the [Medical Biomathematics and Biometrics Commons](#)

Recommended Citation

Law, Philip Mook Wah, "Computer Assisted Electron Spin Resonance Spectral Analysis of Trapped Radicals" (1976). *Loma Linda University Electronic Theses, Dissertations & Projects*. 1868.
<https://scholarsrepository.llu.edu/etd/1868>

This Dissertation is brought to you for free and open access by TheScholarsRepository@LLU: Digital Archive of Research, Scholarship & Creative Works. It has been accepted for inclusion in Loma Linda University Electronic Theses, Dissertations & Projects by an authorized administrator of TheScholarsRepository@LLU: Digital Archive of Research, Scholarship & Creative Works. For more information, please contact scholarsrepository@llu.edu.

LOMA LINDA UNIVERSITY

Graduate School

COMPUTER ASSISTED ELECTRON SPIN RESONANCE
SPECTRAL ANALYSIS OF TRAPPED RADICALS

by

Philip M.W. Law

A Dissertation in Partial Fulfillment
of the Requirements for the Degree
Doctor of Philosophy in the Field of Biomathematics

June 1976

Each person whose signature appears below certifies that he has read this dissertation and that in his opinion it is adequate, in scope and quality, as a dissertation for the degree Doctor of Philosophy.

Wayne E. Zaugg, Chairman
Wayne E. Zaugg, Associate Professor of Chemistry

C. Duane Zimmerman, Co-Chairman
C. Duane Zimmermann, Assistant Professor of
Biomathematics

Ivan R. Neilsen
Ivan R. Neilsen, Director, Professor of
Biomathematics

Harold G. Rutherford
Harold G. Rutherford, Assistant Professor of
Biomathematics

T. Joe Willey
T. Joe Willey, Associate Professor of Physiology

ACKNOWLEDGEMENTS

I wish to express my sincere appreciation and gratitude to Dr. Wayne Zaugg and Dr. C. Duane Zimmermann for their guidance and support in developing and reporting this study; to Dr. Ivan Neilsen for his interest and support; to Dr. Harold Rutherford and Dr. T. Joe Willey for their advice and encouragement.

Appreciation is expressed for grants-in-aid, laboratory-space, equipments, and research materials from the department of Pharmacology and Physiology. Gratitude is extended to the Scientific Computation Facility - a Biotechnology Research Resource supported in part by NIH Grant RR00276.

I like to pay special tribute to my wife, Mary, for her unending support and encouragement and to my parents for their total support.

ACKNOWLEDGEMENTS

I wish to express my sincere appreciation and gratitude to Dr. Wayne Zaugg and Dr. C. Duane Zimmermann for their guidance and support in developing and reporting this study; to Dr. Ivan Neilsen for his interest and support; to Dr. Harold Rutherford and Dr. T. Joe Willey for their advice and encouragement.

Appreciation is expressed for grants-in-aid, laboratory space, equipments, and research materials from the department of Pharmacology and Physiology. Gratitude is extended to the Scientific Computation Facility - a Biotechnology Research Resource supported in part by NIH Grant RR00276.

I like to pay special tribute to my wife, Mary, for her unending support and encouragement and to my parents for their total support.

Computer programs described in this dissertation have been
documented at the Scientific Computation Facility of Loma Linda University

TABLE OF CONTENTS

	Page
LIST OF FIGURES	vii
CHAPTER I. INTRODUCTION	1
CHAPTER II. THEORY AND PRACTICE OF ESR OF TRAPPED RADICALS	4
CHAPTER III. COMPUTER-ASSISTED ANALYSIS OF ESR SPECTRA	14
A. Introduction	14
B. Experiments	16
C. Computer-Assisted Spectral Analysis	20
D. Experimental Data and Spectral Analysis	21
1. Observed Spectra	21
2. Spectral Analysis	21
CHAPTER IV. COMPUTER PROGRAMS FOR SPECTRAL ANALYSIS	38
A. The Main Program For Spectral Analysis	38
B. Major Subroutine	40
1. Subroutine ESRDIS	40
2. Subroutine ESRSTR	40
3. Subroutine ESRSLP	40
4. Subroutine ERSUM	41
5. Subroutine ESRINV	41
6. Subroutine XSCALE	41
7. Subroutine ERSRHF	45
8. Subroutine YSCALE	45
9. Subroutine ERSRMO	45

	Page
10. Subroutine ESRCPY	45
11. Subroutine SCOPX	45
12. Subroutine CNTLTI	45
C. Linkage Program	47
1. ESRSCN	49
2. ESRTRA	49
3. ESRDIX	49
4. PLESR	49
a. The Main Program	49
b. Subroutine ESR	49
c. Subroutine ESRSPC	52
CHAPTER V. SUMMARY AND CONCLUSIONS	55
A. Free Radicals in Gamma-irradiated Hemimellitic Acid Dihydrate Single Crystal	55
B. Computer-Assisted ESR Spectral Analysis	61

REFERENCES

Figure		Page
II - 1	ENERGY LEVELS AND HIGH FIELD TRANSITIONS IN VARYING MAGNETIC FIELD FOR $S = 1/2$ AND $I = 1/2$ SYSTEM FOR AN ARBITRARY ORIENTATION	7
II - 2	PRINCIPAL AXES OF A R_1R_2CH RADICAL WITH TYPICAL PRINCIPAL HYPERFINE COUPLING CONSTANTS	12
III - 1	MORPHOLOGY OF SINGLE CRYSTAL OF HEMIMELLITIC ACID DIHYDRATE	17
III - 2	BLOCK DIAGRAM OF LLU ESR SPECTROMETER	19
III - 3	ESR SPECTRUM WITH EXTERNAL FIELD ALONG X AXIS	22
III - 4	ESR SPECTRUM WITH EXTERNAL FIELD ALONG Y AXIS	22
III - 5	ESR SPECTRUM WITH EXTERNAL FIELD ALONG Z AXIS	22
III - 6	ESR SPECTRUM WITH SIMPLE ABSORPTION LINE SHAPE	23
III - 7	ESR SPECTRUM WITH ABSORPTION LINES SUBSTRUCTURES ...	23
III - 8	ESR SPECTRUM SHOWING CENTRAL CONTRIBUTION OF WING STRUCTURES	24
III - 9	ESR SPECTRUM SHOWING CENTRAL CONTRIBUTION OF WING STRUCTURES	24
III - 10	ESR SPECTRUM OF DEUTERATED CRYSTAL	25
III - 11	EFFECT OF POWER SATURATION	26
III - 12	INTERPRETATION OF AN ESR SPECTRUM	28
III - 13	ANGULAR VARIATION OF HYPERFINE SPLITTINGS OF AN ALPHA PROTON	30
III - 14	ANGULAR VARIATION OF HYPERFINE SPLITTINGS OF A METHYLENE PROTON	31
III - 15	ANGULAR VARIATION OF HYPERFINE SPLITTINGS OF A METHYLENE PROTON	32
III - 16	SUPERIMPOSED EXPERIMENTAL AND SIMULATED ESR SPECTRA.	36
IV - 1	FLOWCHART FOR MAIN PROGRAM PLSPEC	39
IV - 2	INTEGRATED ESR SPECTRUM WITH SLANTING BASELINE	42

Figure	Page
IV - 3	ESR SPECTRUM WITH SLANTING BASELINE CORRECTION 42
IV - 4	A SAMPLE ESR SPECTRUM, A 43
IV - 5	A SAMPLE ESR SPECTRUM, B 43
IV - 6	SUMMATION SPECTRUM, A + B 43
IV - 7	DIFFERENCE SPECTRUM, A - B 43
IV - 8	INVERSION OF THE SPECTRUM OF FIGURE IV - 4 44
IV - 9	HORIZONTAL CONTRACTION OF SPECTRUM OF FIGURE IV - 4 TO 1/3 ITS ORIGINAL SPAN 46
IV - 10	HORIZONTAL EXPANSION OF SPECTRUM OF FIGURE IV - 4 BY 3 TIMES 46
IV - 11	TITRATION OF CENTRAL COMPONENTS 48
IV - 12	ESR SPECTRUM WITH CURSOR AND ITS COORDINATES DISPLAYED. 50
IV - 13	INTEGRATED ESR SPECTRUM OF FIGURE IV - 4 51
IV - 14	DIFFERENTIATED ESR SPECTRUM OF FIGURE IV - 4 51
IV - 15	SIMULATED GAUSSIAN ABSORPTION ESR SPECTRUM OF A PROTON INTERACTING WITH 3 EQUIVALENT SPIN 3/2 NUCLEI 53
IV - 16	SIMULATED LORENTZIAN ABSORPTION ESR SPECTRUM OF A PROTON INTERACTING WITH 3 EQUIVALENT SPIN 3/2 NUCLEI 53
IV - 17	SECOND DERIVATIVE OF SPECTRUM IN FIGURE 16 54
IV - 18	FIRST DERIVATIVE OF SPECTRUM IN FIGURE 16 54
V - 1	SIMULATED ESR SPECTRA OF CYCLOHEXADIENYL-TYPE FREE RADICALS DERIVED FROM GAMMA-IRRADIATED HEMIMELLITIC ACID OR MONODEUTEROHEMIMELLITIC ACID SINGLE CRYSTALS AT AN ARBITRARY ORIENTATION 57

CHAPTER I

INTRODUCTION

Electron Spin Resonance Spectroscopy (ESR) is a spectroscopic method of detecting the presence of unpaired electrons in atoms, ions, molecules or molecular fragments. Some atoms or molecules possess unpaired electrons naturally. Others derive their unpaired electrons from radiation damage or other chemical or physical means. These are called free radicals. All substances possessing unpaired electrons are paramagnetic. ESR is applicable only to paramagnetic materials.

When the orbit of an unpaired electron embraces an atom which has a nucleus with spin, there will be interactions between the electron and nuclear magnetic moments. They are recorded as hyperfine structures in ESR spectra. From these hyperfine structures, precise information of the structure of the radicals and the distribution of the odd electron can be deduced. These hyperfine structures consist of anisotropic and isotropic components. The isotropic part is independent of the orientation of the radicals with respect to the direction of the external magnetic field while the anisotropic part is directionally dependent.

Since about 1958, there has been explosive expansion in the investigation of oriented radicals. The subject has been reviewed by Morton (1). Recently Farrach and Poole (2) presented an overall theoretical treatment and the application of the theory to the experimental situation.

The analysis of ESR spectra of oriented radicals is generally quite complicated, particularly with anisotropy. The use of a high-speed digital computer can assist greatly in the process of spectral parameter and radical identification. This is done by programmed spectral resolution enhancement, identification and extraction of pertinent data, numerical computation and spectral simulations. The simulation of experimental spectra with parameters derived from spectral analysis or a theoretical model is considered important supportive evidence for the complete identification of a radical.

There are many reports on the utilization of computers to various aspects of ESR spectroscopy. Kertez and Wolfs (3), for example, reported a time-sharing, on-line computer system for the analysis of ESR spectra of organic free radicals. Klopfenstein, Jost and Griffith (4) described a dedicated computer in ESR spectroscopy. Many other reports (5-8) dealt with specific techniques of ESR spectral analysis.

A set of general purpose computer programs is written in this study to assist in the analysis of complex spectra. Some special programs and subroutine are also included for the analysis of anisotropic ESR spectra of oriented free radicals. An interactive approach is adopted, taking advantage of the computer and graphics terminals of the Scientific Computation Facility at Loma Linda University. The programs are readily adaptable to other areas of interest involving spectral analysis.

As an application, the programs are used to assist in the study of the free radicals in gamma-irradiated single crystals of 1,2,3-benzene

tricarboxylic acid dihydrate.

Chapter II, which follows this introduction, outlines the theory of ESR. The effective spin Hamiltonian of a free radical in which one unpaired electron interacts with one proton is described. The eigenfunctions and eigenvalues of the Hamiltonian are given. Mathematical methods to obtain the principal values of the hyperfine interaction tensor are discussed.

Chapter III reports the investigation of free radicals in gamma-irradiated single crystals of 1,2,3-benzene tricarboxylic acid dihydrate.

Chapter IV is a general description of the computer programs written to assist in spectral analysis. Brief descriptions are given of the twelve major subroutines of the main analysis program. Four linkage programs are also described.

Chapter V is a conclusion on the application of the computer for ESR spectral analysis. Further research and development are suggested.

CHAPTER II

THEORY AND PRACTICE OF ESR OF TRAPPED RADICALS

The spin Hamiltonian for a free radical in which one unpaired electron interacts with one proton is

$$H = \beta \bar{H} \cdot \bar{g} \cdot \bar{S} + \bar{S} \cdot \bar{A} \cdot \bar{I} + g_N \beta_N \bar{H} \cdot \bar{I}$$

Where β is the Bohr magneton, \bar{S} is the electron spin operator, \bar{g} is the spectroscopic splitting factor, \bar{A} is the hyperfine interaction tensor, \bar{H} the external magnetic field, and \bar{I} is the nuclear spin operator. The three terms on the right hand side of the equation are the Electron Zeeman, Hyperfine interaction, and Nuclear Zeeman terms respectively.

Since Organic free radicals show relatively little g-tensor anisotropy, the g-tensor can be regarded as a scalar. Thus we have for the Hamiltonian

$$H = g\beta \bar{H} \cdot \bar{S} + \bar{S} \cdot \bar{A} \cdot \bar{I} + g_N \beta_N \bar{H} \cdot \bar{I}$$

Assuming that the nuclear Zeeman effect is small and negligible we have

$$H = g\beta \bar{H} \cdot \bar{S} + \bar{S} \cdot \bar{A} \cdot \bar{I}$$

$$= g\beta [H_x, H_y, H_z] \cdot \begin{bmatrix} S_x \\ S_y \\ S_z \end{bmatrix} + [S_x, S_y, S_z] \cdot \begin{bmatrix} A_{xx} & A_{xy} & A_{xz} \\ A_{yx} & A_{yy} & A_{yz} \\ A_{zx} & A_{zy} & A_{zz} \end{bmatrix} \cdot \begin{bmatrix} I_x \\ I_y \\ I_z \end{bmatrix}$$

where x, y, z are an orthogonal set of axes based on the morphology of the single crystal.

Expanding the Hamiltonian gives

$$H = g\beta H_x \hat{S}_x + g\beta H_y \hat{S}_y + g\beta H_z \hat{S}_z + S_x A_{xx} I_x + S_x A_{xy} I_y + \dots + S_z A_{zz} I_z$$

Let a, b, c be the orthogonal laboratory axes. The direction cosines of a, b, c with respect to x, y, z are (l_a, m_a, n_a) , (l_b, m_b, n_b) , and (l_c, m_c, n_c) .

When the Zeeman energy is relatively large, so that the hyperfine interaction causes no mixing of the zero order electron spin states, we can expand the Hamiltonian in the a, b, c axes and dropping the terms in S_a and S_b , which are off diagonal in M_s , and obtain

$$H = g\beta H_c S_c + P_x S_c I_x + P_y S_c I_y + P_z S_c I_z$$

Where

$$P_x = l_c A_{xx} + m_c A_{yx} + n_c A_{zx}$$

$$P_y = l_c A_{yy} + m_c A_{zy} + n_c A_{xy}$$

$$P_z = l_c A_{zz} + m_c A_{xz} + n_c A_{yz}$$

The matrix of the Hamiltonian H , $\langle M_{S_I} M_I | H | M_{S_I} M_I \rangle$, for $M_S = M_I = 1/2$

is

	$ \alpha\alpha\rangle$	$ \alpha\beta\rangle$	$ \beta\alpha\rangle$	$ \beta\beta\rangle$
$\langle\alpha\alpha $	$1/2g\beta H_C + 1/4P_Z$	$1/4(P_X - iP_Y)$	0	0
$\langle\alpha\beta $	$1/4(P_X + iP_Y)$	$1/2g\beta H_C - 1/4P_Z$	0	0
$\langle\beta\alpha $	0	0	$-1/2g\beta H_C - 1/4P_Z$	$-1/4(P_X - iP_Y)$
$\langle\beta\beta $	0	0	$1/4(P_X + iP_Y)$	$-1/2g\beta H_C + 1/4P_Z$

From which we obtain the eigenfunctions

$$\psi_1 = \{2R(R-P_Z)\}^{-\frac{1}{2}} \{ (P_X - iP_Y) |\alpha\alpha\rangle + (R-P_Z) |\alpha\beta\rangle \}$$

$$\psi_2 = \{2R(R+P_Z)\}^{-\frac{1}{2}} \{ (P_X - iP_Y) |\alpha\alpha\rangle - (R+P_Z) |\alpha\beta\rangle \}$$

$$\psi_3 = \{2R(R+P_Z)\}^{-\frac{1}{2}} \{ (P_X - iP_Y) |\beta\alpha\rangle - (R+P_Z) |\beta\beta\rangle \}$$

$$\psi_4 = \{2R(R-P_Z)\}^{-\frac{1}{2}} \{ (P_X + iP_Y) |\beta\alpha\rangle + (R-P_Z) |\beta\beta\rangle \}$$

$$\text{where } R = \{ P_X^2 + P_Y^2 + P_Z^2 \}^{\frac{1}{2}}$$

and the eigen values

$$E_1 = 1/2 g\beta H_C + 1/4 R$$

$$E_2 = 1/2 g\beta H_C - 1/4 R$$

$$E_3 = -1/2 g\beta H_C + 1/4 R$$

$$E_4 = -1/2 g\beta H_C - 1/4 R$$

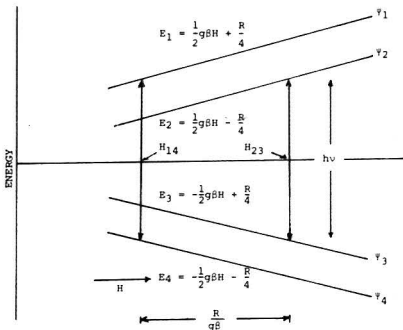


FIGURE II - 1 ENERGY LEVELS AND HIGH FIELD TRANSITIONS IN VARYING MAGNETIC FIELD FOR $S = \frac{1}{2}$ AND $I = \frac{1}{2}$ SYSTEM FOR AN ARBITRARY ORIENTATION.

Transitions of electrons at different energy levels are induced by an alternating field perpendicular to the applied magnetic field and we find the transition probabilities

$$\{ \langle \psi_1 | S_a | \psi_4 \rangle \}^2 = \{ \langle \psi_2 | S_a | \psi_3 \rangle \}^2 = 1$$

$$\{ \langle \psi_2 | S_a | \psi_4 \rangle \}^2 = \{ \langle \psi_1 | S_a | \psi_3 \rangle \}^2 = 0$$

In practice the microwave frequency is held constant and the external magnetic field is varied. Fig. II - 1 shows the transition from E_1 to E_4 occurs at lower field, H_{14} , and the transition from E_2 to E_3 occurs at a higher field, H_{23} .

Since the microwave frequency is constant, the transition energies are

$$h\nu = E_1 - E_4 = g\beta H_{14} + 1/2R$$

and

$$h\nu = E_2 - E_3 = g\beta H_{23} - 1/2R$$

Hence the ESR spectrum comprises two lines of equal intensity with a field separation of

$$\Delta H = H_{23} - H_{14} = \frac{R}{g\beta}$$

Writing R in full, dropping the subscripts, c, for the direction cosines we see that

$$\begin{aligned} R^2 &= (\hat{l} \cdot \hat{A}) \cdot (\hat{A} \cdot \hat{l}) \\ &= \hat{l} \cdot (\hat{A})^2 \cdot \hat{l} \\ &= \hat{l} \cdot \hat{T} \cdot \hat{l} \end{aligned}$$

where $\hat{l} = [l, m, n,]$ is the direction cosine vector

$$\text{and } \hat{T} = \hat{A}^2$$

$$\text{i.e. } \begin{bmatrix} T_{xx} & T_{xy} & T_{xz} \\ T_{yx} & T_{yy} & T_{yz} \\ T_{zx} & T_{zy} & T_{zz} \end{bmatrix} = \begin{bmatrix} A_{xx} & A_{xy} & A_{yz} \\ A_{yx} & A_{yy} & A_{yz} \\ A_{zx} & A_{zy} & A_{zz} \end{bmatrix} \cdot \begin{bmatrix} A_{xx} & A_{xy} & A_{xz} \\ A_{yx} & A_{yy} & A_{yz} \\ A_{zx} & A_{zy} & A_{zz} \end{bmatrix}$$

Experimentally, we mount the crystal along three orthogonal axes and rotate about each axis at fixed intervals of say 10° with the external field perpendicular to the axis of rotation. For example, if we rotate the crystal about the Z-axis and specify the direction of the

field in the xy-plane by the angle θ which it makes with the x-axis, we have

$$l = \cos \theta \quad m = \sin \theta \quad n = 0$$

and

$$R^2(\theta) = (T_{xx} \cos^2\theta + T_{yy} \sin^2\theta + 2T_{xy} \sin\theta \cos\theta)$$

The least square procedure is employed to fit the experimental curve of $R^2(\theta)$ versus θ , and the elements of the \bar{T} tensor are obtained.

The \bar{T} matrix is diagonalized and square roots of the diagonal values are the principal hyperfine coupling constants, A_{XX} , A_{YY} and A_{ZZ} , where X, Y, Z are the principal axes of the free radical. Since the principal constants are each the sums of an anisotropic dipolar interaction and an isotropic contact interaction tensor, we have

$$\begin{bmatrix} A_{XX} & 0 & 0 \\ 0 & A_{YY} & 0 \\ 0 & 0 & A_{ZZ} \end{bmatrix} = \begin{bmatrix} A_d & 0 & 0 \\ 0 & B_d & 0 \\ 0 & 0 & C_d \end{bmatrix} + \begin{bmatrix} a & 0 & 0 \\ 0 & a & 0 \\ 0 & 0 & a \end{bmatrix}$$

where a is the isotropic Fermi contact interaction constant.

Hyperfine splittings due to the isotropic interaction of a nucleus directly attached to an atom with an unpaired electron is proportional to the electron spin density at the atom (1). By comparing spin densities determined from ESR spectra of a free radical with those calculated for various proposed alternatives, it is possible to ascertain the correct radical species, or at least narrow the possibilities.

Expressed in polar coordinates, the dipolar interaction constants are

$$A_d = C \int_{\epsilon} \frac{\rho(r) (1-3\sin^2\theta \cos^2\phi) d\tau}{|\vec{r}|^3}$$

$$B_d = C \int_{\epsilon} \frac{\rho(r) (1-3\sin^2\theta \sin^2\phi) d\tau}{|\vec{r}|^3}$$

$$C_d = C \int_{\epsilon} \frac{(1-3\cos^2\theta) d\tau}{|\vec{r}|^3}$$

where $C = g\beta g_N \beta_N / h$

In these equations, h is Planck's constant, g_N is the nuclear g-factor, β_N is the nuclear magneton, θ is the polar angle, ϕ is the azimuthal angle, $\rho(r)$ is the electron density function with the origin at the proton, \vec{r} is the vector denoting the location of the electron with respect to the proton, ϵ indicates a small region around the nucleus with a radius of the order of $(h/2\pi mc) = 4 \times 10^{-11}$ cm which is excluded from the integration.

In general the principal axes, X, Y, Z, do not coincide with the crystal axes, x, y, z. Therefore the dipolar interaction tensor can be written

$$g\beta g_N \beta_N \begin{bmatrix} \left\langle \frac{r^2 - 3x^2}{r^5} \right\rangle & - \left\langle \frac{3xy}{r^5} \right\rangle & - \left\langle \frac{3xz}{r^5} \right\rangle \\ - \left\langle \frac{3xy}{r^5} \right\rangle & \left\langle \frac{r^2 - 3y^2}{r^5} \right\rangle & - \left\langle \frac{3yz}{r^5} \right\rangle \\ - \left\langle \frac{3xz}{r^5} \right\rangle & - \left\langle \frac{3yz}{r^5} \right\rangle & \left\langle \frac{r^2 - 3z^2}{r^5} \right\rangle \end{bmatrix}$$

The angular brackets imply an average taken over the electron wave function, as the electron is not fixed in space. We see that the matrix is symmetric and it has a zero trace. Since the trace of a matrix is preserved under unitary transformation, we have

$$A_{XX} + A_{YY} + A_{ZZ} = (A_d + B_d + C_d) + 3a = 3a$$

Hence,

$$a = \frac{1}{3} (A_{XX} + A_{YY} + A_{ZZ})$$

The transformation that diagonalizes the \bar{T} matrix gives the direction cosines of the principal hyperfine axes X,Y,Z with respect to the crystal reference axes x,y,z, that is

$$\begin{bmatrix} l_{xX} & l_{xY} & l_{xZ} \\ l_{yX} & l_{yY} & l_{yZ} \\ l_{zX} & l_{zY} & l_{zZ} \end{bmatrix} \begin{bmatrix} A_{XX} & 0 & 0 \\ 0 & A_{YY} & 0 \\ 0 & 0 & A_{ZZ} \end{bmatrix} \begin{bmatrix} l_{xX} & l_{yX} & l_{zX} \\ l_{xY} & l_{yY} & l_{zY} \\ l_{xZ} & l_{yZ} & l_{zZ} \end{bmatrix} = \begin{bmatrix} A_{xx} & A_{xy} & A_{xz} \\ A_{yx} & A_{yy} & A_{yz} \\ A_{zx} & A_{zy} & A_{zz} \end{bmatrix}$$

It is possible to relate these principal hyperfine coupling constants and their principal directions to the structure and orientation of the free radical in the crystal. Theoretical calculations (9,10) show that the principal axes for a trigonal carbon atom with an unpaired electron in a $2P_z$ orbital normal to the radical plane are related to the C-H bond direction. The direction of the minimum principal coupling constant is along the C-H bond whereas that of the intermediate principal coupling constant is perpendicular to the radical plane, i.e. parallel to the P_z orbital. See Figure II - 2. Thus the direction cosines specify

the orientation of the free radical with respect to the crystal axis system.

When more than one nuclei with spin interact with an unpaired electron, complex hyperfine patterns may occur. In case of the equivalence of the interacting nuclei, ESR spectra will show absorption lines bearing simple binomial ratios (22). For example, two equivalent protons give three lines of relative intensities 1:2:1; three equivalent protons, such as those in a rapidly rotating methyl group, yield four lines of relative intensities 1:3:3:1. Thus the number and relative intensities of the ESR spectral lines are often the first clue to the identification of a free radical.

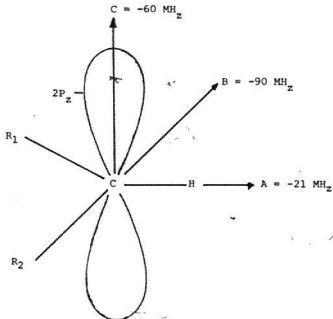


FIGURE II - 2 PRINCIPAL AXES OF A R_1R_2CH RADICAL WITH TYPICAL PRINCIPAL HYPERFINE COUPLING CONSTANTS

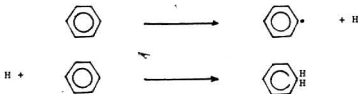
Many excellent references (11-15) are available for further development of the theory and practice of electron spin resonance spectroscopy.

CHAPTER III

COMPUTER-ASSISTED ANALYSIS OF ESR SPECTRA

A. INTRODUCTION :

Free radicals produced by irradiation of benzene and its derivatives have been studied by a number of investigation. Ohnishi, Tanei and Nitta (16) studied polycrystalline benzene and some of its mono- and di-substituted derivatives after gamma-irradiation at -196°C . They proposed that free radicals were produced by both hydrogen abstraction and hydrogen addition on the benzene ring. For example, cyclohexaldienyl and phenyl radicals are formed when crystalline benzene is irradiated.



The cyclohexaldienyl radical gives rise to an ESR spectrum that consists of a triplet (splitting 47.5G) with a quartet (splitting 10.4G), each quartet showing further triplet splittings of approximately 2.5G. The structure was designated the TQT structure. The phenyl radical gives rise to a singlet of about 25G line width.

Fessenden and Schuler (17) studied irradiated solid benzene at and below 0°C. They disagreed on the TQT structure interpretation of the cyclohexaldienyl free radical. Their arguments were based on ESR spectral asymmetry and the unequal spacing of various group components. Kasai, Hedaja and Whipple (18) studied phenyl radicals by the photolysis of phenyl iodide in an argon matrix at 4°K. The unpaired electron was found to be localized in the nonbonding sigma orbital centered at the 1 carbon with isotropic coupling constants: $A_{ortho} = 17.4 \pm 0.1G$, $A_{meta} = 5.9 \pm 0.1G$ and $A_{para} = 1.9 \pm 0.1G$.

Campbell and Turner (19) investigated many gamma-irradiated solid substituted benzenes. Not all compounds gave cyclohexaldienyl-type ESR spectra. They found that cyclohexaldienyl-type radicals are more readily formed when solid substituted benzenes were irradiated at room temperature. Also cyclohexaldienyl-type of radicals were found to be more readily formed from 1,3 than 1,2- or 1,4- disubstituted benzenes.

Eiben and Schuler (20) studied carboxylated cyclohexaldienyl radicals in aqueous solution. For 1,2,3- benzene tricarboxylate acid (hemimellitic acid), they reported two radical species. Adduct hydrogen at the meta position with respect to the central carboxylate group, gives a hyperfine coupling of 43.99 gauss. Hyperfine coupling constants for the protons adjacent and meta to the adduct hydrogen at the para position, to the central carboxylate group, gives a hyperfine coupling constant of 44.95 gauss. The other two ring protons were found to be equivalent with a coupling constant of 8.29 gauss.

Mo and Adman (21) reported crystallographic studies of 1,2,3-benzene tricarboxylic acid dihydrate crystal. Table III - 1 lists the crystallographic data of hemimellitic acid dihydrate crystals.

It is the purpose of this study to investigate free radicals in gamma-irradiated single crystal of hemimellitic acid dihydrate.

B. EXPERIMENTS:

Powdered hemimellitic acid was dissolved in distilled water to make a saturated solution. Under slow evaporation, hemimellitic acid crystallized out at the bottom of the container. Deuterated crystals were grown in similar manner with 99.5% pure heavy water, D_2O , as solvent.

Figure III - 1 shows the morphology of a single crystal hemimellitic acid with designated crystallographic axes and faces based on external symmetry.

Crystals each of approximate size of $3\text{mm} \times 4\text{mm} \times 5\text{mm}$ were gamma-irradiated at room temperature in a Gamma Cell each with dosage of about 5Mr at a rate of 7.64×10^4 rad per hour.

Irradiation turns the color of the crystal pinkish. Each crystal was oriented by an optical method based on the external symmetry of the crystal. Each crystal was mounted on top of a goniometer which provided rotation about three orthogonal axes. The goniometer itself was mounted on an optical bench. A point source arc lamp was used to project the shadow of the crystal on a grid paper. Crystallographic axes were aligned to within 1 degree. Once aligned, each crystal was glued to a polystyrene rod approximately 8 in. long, with the desired crystallographic axis parallel

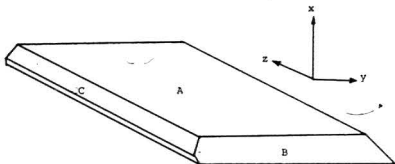


FIGURE III - 1 MORPHOLOGY OF SINGLE CRYSTAL OF HEMIMELLITIC ACID DIHYDRATE

TABLE III - 1 HEMIMELLITIC ACID DIHYDRATE SINGLE CRYSTAL DATA

CRYSTAL SYSTEM	TRICLINIC
Angles between axes	$\alpha = 100.70 \pm .02 \text{ }^{\circ}$ $\beta = 88.10 \pm .02 \text{ }^{\circ}$ $\gamma = 106.46 \pm .02 \text{ }^{\circ}$
Lengths of axes	$a = 8.728 \pm .004 \text{ } \text{\AA}$ $b = 9.118 \pm .004 \text{ } \text{\AA}$ $c = 7.086 \pm .004 \text{ } \text{\AA}$
Molecules per cell	2
Space group	$P \bar{1}$

to the axis of the rod.

ESR spectra were recorded at room temperature with external magnetic field in the three orthogonal reference planes xy , yz , and xz , see reference axes in Figure III - 1. An X-band spectrometer of conventional design with 100 KHz modulation was used. Figure III - 2 is a block diagram of the LLU ESR spectrometer. ESR spectra were recorded at 10 degree intervals in each plane by successive rotation of the crystal. The ESR spectrometer was most commonly operated with field modulation of approximately one gauss and sensitivities of 20 mV. All spectra were taken with a magnetic field sweep of 200 gauss. Scan rate was 0.4 gauss per second.

Each ESR spectrum was traced on graph paper by an x-y plotter, and at the same time it was recorded on an Ampex SP-300 7 channel magnetic tape recorder. Two channels were used. Channel one recorded the spectrum from the spectrometer. Channel two recorded a trigger pulse from a hand operated pulse generator prior to each magnetic scan of the spectrum. Data on magnetic tape were digitized at 28 data points per second and stored in LINCTAPE via a Digital Equipment Corporation PDP-12 computer. Digitization was accomplished by the PDP-12 program CATACALE. The trigger pulse recorded on channel two of the tape recorder was used to initiate the digitization of each spectrum. There were 1024 data points per ESR spectrum.

Information stored on LINCTAPE was transcribed on high density 6250 bpi Scotch tape to be analyzed at the Scientific Computation Facility. For random access and spectral analysis, data on magnetic tape was stored on disc at the Facility.

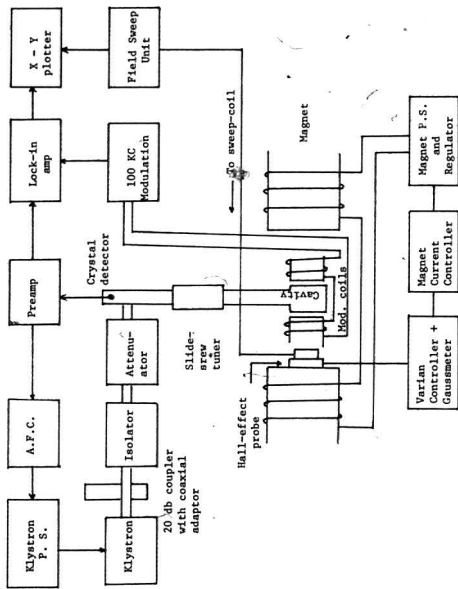


FIGURE III - 2 BLOCK DIAGRAM OF LLU ESR SPECTROMETER

C. COMPUTER-ASSISTED SPECTRAL ANALYSIS :

After the main program, PLSPEC, was compiled and executed, interactive analysis procedures were carried out by successive entering of operating codes and necessary parameters. Typically, an ESR spectrum was called from disc and displayed at the CRT terminal by entering the file and record number of the spectrum. If the spectrum was 180° out of phase with other spectra it was inverted. The smoothing procedure was applied when needed. A cursor was programed to trace along the spectrum. At appropriate points, the enabling of a computer sense switch stopped the trace and caused the display of the coordinates of the stopping points. The field values were recorded in a note book. Hyperfine coupling constants were obtained from these values. Integration was sometimes carried out to ascertain the ratio of line intensities. The ESR spectrum was recorded as a first derivative curve. A differentiation operation gave the second derivative which often helped to ascertain the magnetic field value of an absorption line. Any baseline slanting as the result of integration or differentiation was corrected.

Data recorded in the notebook were used for the simulation of the spectrum. This helped to ascertain correct interpretation of the hyperfine splittings. To compare this spectrum with the experimental one, both spectra were displayed on the CRT terminal together. Shifting and scaling of one spectrum in both the x and y directions might be needed. This would bring the two spectra into close fit.

The central components of the spectrum was titrated with high and low field structures. This was intended to expose superimposed hyperfine structure due to different radical species. Further details are discussed in the next section.

D. EXPERIMENTAL DATA AND SPECTRAL ANALYSIS :

1. Observed Spectra

Upon examining the whole set of ESR spectra, a prominent feature of two lateral doublets and a central line group is apparent. They bore an intensities ratio of close to 1:2:1. See Figures III - 3 to III - 5. In certain orientations, each absorption line further decomposed into sub-structures. See Figures III-6 and III-7.

The similarity of the line shapes between the lateral doublets and lines in the central components indicated that the doublets had central contributions. See Figures III-8 and III-9.

Deuterated crystals show similar spectra with better resolution. More auxiliary lines occurred between the lateral doublets and the central components. See Figure III - 9 & 10. Since the extent and location of deuteration on the crystal molecules were not determined, investigation on these auxiliary lines were not made.

Power saturation reduces the relative intensities of outer doublets and their corresponding central components. However, the spectrum still shows rather complicated pattern. See Figure III - 11.

2. Spectral Analysis

The 1:2:1 ratio between the lateral doublets and the central components can be interpreted as due to anisotropic hyperfine interactions with two nearly equivalent protons. In general the two lateral doublets show the same shape whereas the central line group differ somewhat, indicating that equivalence is not quite achieved.



FIGURE III - 3 ESR SPECTRUM WITH EXTERNAL FIELD ALONG X AXIS



FIGURE III - 4 ESR SPECTRUM WITH EXTERNAL FIELD ALONG Y AXIS



FIGURE III - 5 ESR SPECTRUM WITH EXTERNAL FIELD ALONG Z AXIS



FIGURE III - 6 ESR SPECTRUM WITH SIMPLE ABSORPTION LINE SHAPE



FIGURE III - 7 ESR SPECTRUM WITH ABSORPTION LINES SUBSTRUCTURES



FIGURE III - 8 ESR SPECTRUM SHOWING CENTRAL CONTRIBUTION OF WING STRUCTURES

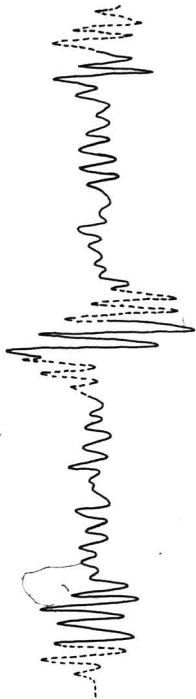


FIGURE III - 9 ESR SPECTRUM SHOWING CENTRAL CONTRIBUTION OF WING STRUCTURES



FIGURE III - μ ESR SPECTRUM OF DEUTERATED CRYSTAL



(a) LOW - MICROWAVE POWER



(b) HIGH MICROWAVE POWER

FIGURE III - 11 EFFECT OF POWER SATURATION ON AN ESR SPECTRUM

Figure III - 12 shows a possible interpretation of a typical spectrum. The two larger and almost equal hyperfine splittings show relatively small anisotropy. However, the hyperfine splitting that gives rise to the doublet is fairly anisotropic. The smallest hyperfine splitting is not resolvable in most orientations.

These results strongly suggest hyperfine interactions with two protons of a methylene group. A hydrogen atom has been added to a carbon atom of the aromatic ring. Thus the carbon atom sp^2 orbital transforms to a sp^3 hybridization. The doublet splitting is the result of the hyperfine interactions between an aromatic ring proton and the remaining benzene ring pi-orbital. The poorly resolved splitting is contributed by another ring proton.

Cyclohexadienyl-type radicals resulting from hydrogen addition at the 4 or 6 positions meet the above criteria.



Consider the case of hydrogen addition at the 4 position, the two methylene protons on carbon 4 are almost equivalent. They are beta protons, hence they exhibit small anisotropy. Three hyperconjugation structures can be written.

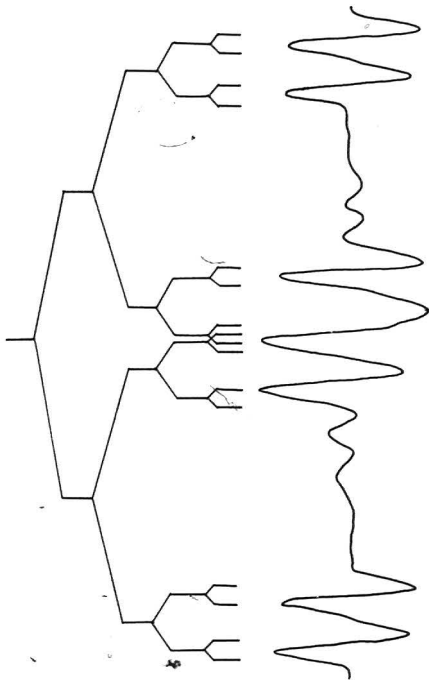
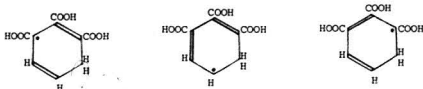
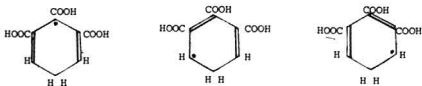


FIGURE III - 12 INTERPRETATION OF AN ESR SPECTRUM



The spin density at C_5 is higher than that of C_6 . Therefore, H_5 gives rise to the doublet splitting while H_6 gives rise to the smallest hyperfine splitting.

An alternative free radical resulted in hydrogen addition at the C_5 position has the following three hyperconjugate structures:



These strongly suggest equal electron spin density at the C_4 and C_6 positions. Near equivalence of H_4 and H_6 would show triplet splittings with relative intensities ratio close to 1:2:1 at the high and low field positions. However, such feature is not observed in any of the ESR spectra. It is concluded that hydrogen addition at the C_5 proton is insignificant.

Figure III - 13 to 15 show the angular variation of the three measurable hyperfine splitting constants. Least square procedure is applied to the Data. Solid lines in the figures join the computed values. The square of the hyperfine interaction tensor of the proton at C_5 is also obtained by the least square procedure. Expressed in megahertz unit it is :

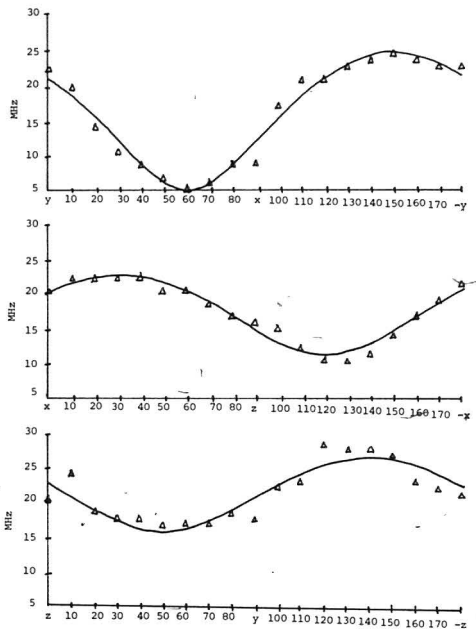


FIGURE III - 13 ANGULAR VARIATION OF HYPERFINE SPLITTINGS OF AN ALPHA PROTON

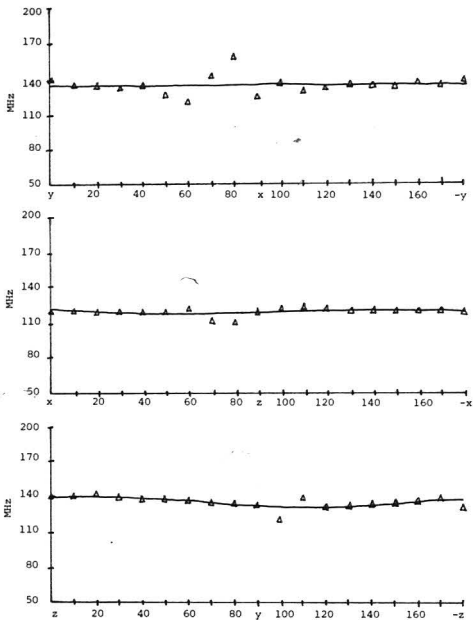


FIGURE III - 14 ANGULAR VARIATION OF HYPERFINE SPLITTINGS OF A METHYLENE PROTON

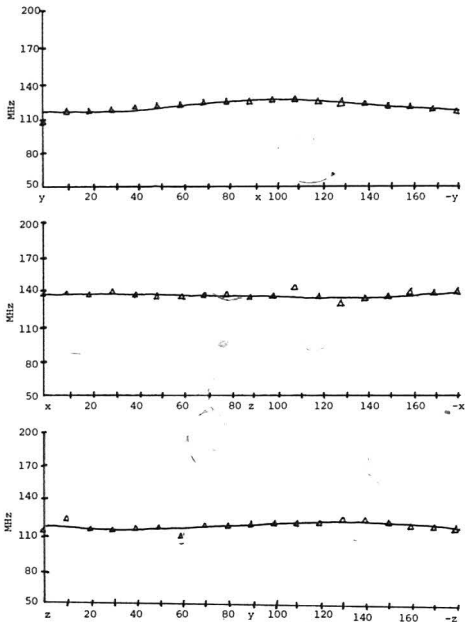


FIGURE III - 15 ANGULAR VARIATION OF HYPERFINE SPLITTINGS OF A METHYLENE PROTON

Ap

$$\begin{bmatrix} 340.51 & -329.25 & 220.27 \\ -329.25 & 676.72 & -274.93 \\ 220.27 & -274.93 & 698.92 \end{bmatrix}$$

It is diagonalized to give :

$$\begin{bmatrix} 134.05 & 0 & 0 \\ 0 & 432.10 & 0 \\ 0 & 0 & 1150.23 \end{bmatrix}$$

Taking the square roots of the diagonal matrix elements gives the tensor of principal hyperfine coupling constants.

$$\begin{bmatrix} -11.58 & 0 & 0 \\ 0 & -20.79 & 0 \\ 0 & 0 & -33.92 \end{bmatrix}$$

The negative signs are imposed by spin density distribution considerations (22). The tensor is resolved into anisotropic and isotropic parts :

$$\begin{bmatrix} -11.58 & 0 & 0 \\ 0 & -20.79 & 0 \\ 0 & 0 & -33.92 \end{bmatrix} = \begin{bmatrix} -10 & 0 & 0 \\ 0 & +1.31 & 0 \\ 0 & 0 & -11.82 \end{bmatrix} + \begin{bmatrix} -2.10 & 0 & 0 \\ 0 & -22.10 & 0 \\ 0 & 0 & -22.10 \end{bmatrix}$$

The direction cosines of the principal axes with respect to the crystal x,y,z axes are :

$$\begin{bmatrix} -0.8750 & -0.4344 & 0.1097 \\ 0.2189 & -0.5633 & -0.7898 \\ 0.4350 & -0.6588 & 0.1613E \end{bmatrix}$$

The direction associated with the intermediate principal coupling constant is parallel to the carbon $2P_z$ orbital. From the direction cosines corresponding to this axis, it is expected that it makes angles of $77^{\circ}22'$, $144^{\circ}18'$, and $128^{\circ}48'$ with the crystal x,y,z axes, respectively. Assuming no major conformational change of the benzene ring due to radiation, the P_z orbital of C_5 should be parallel to the normal of the benzene ring. From crystallographic data the direction cosines of this normal with respect to the crystal axes can be evaluated. Theoretically these direction cosines should agree. Due to the difficulties of correlating the crystal morphology with the unit cell orientation. Such agreement has not been determined.

The hyperfine interaction tensor of one of the methylene proton is found to be :

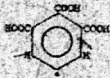
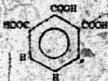
$$\begin{bmatrix} 122.36 & 0 & 0 \\ 0 & 121.04 & 0 \\ 0 & 0 & 116.48 \end{bmatrix} = \begin{bmatrix} 2.40 & 0 & 0 \\ 0 & 11.08 & 0 \\ 0 & 0 & -1.48 \end{bmatrix} + \begin{bmatrix} 119.96 & 0 & 0 \\ 0 & 119.96 & 0 \\ 0 & 0 & 119.96 \end{bmatrix}$$

The other methylene proton hyperfine interaction tensor is :

$$\begin{bmatrix} 177.51 & 0 & 0 \\ 0 & 138.77 & 0 \\ 0 & 0 & 139.27 \end{bmatrix} = \begin{bmatrix} -3.00 & 0 & 0 \\ 0 & 1.25 & 0 \\ 0 & 0 & 1.75 \end{bmatrix} + \begin{bmatrix} 177.54 & 0 & 0 \\ 0 & 137.54 & 0 \\ 0 & 0 & 137.54 \end{bmatrix}$$

The average value of the isotropic hyperfine interaction constants of the methylene protons in units of gauss is 45.99 gauss, and that of the C_3 proton is 86 gauss. They agree fairly well with published values of 43.99 gauss and 86.07 gauss respectively (20). Simulated spectra based on measured values fit well with experimental spectra. See figure III - 16.

One of the sources of the adduct hydrogen is the ring proton of a neighbor molecule. If this the case, phenyl-type free radicals are formed:



It is expected phenyl-type radicals would contribute to the central components of the ESR spectra. Titration of central components with lateral doublets structures was done with UNIVAC series 20 computer for ESR spectra. The lateral doublets on the high and low field positions were shifted to the center by the amounts equal to measured methylene protons hyperfine splittings. They were subtracted from the central components. The resultant spectra are quite complicated; they are not analyzed

Experimental

..... Simulated

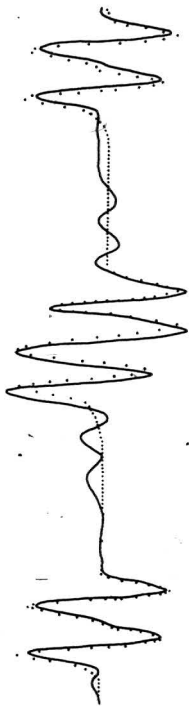


FIGURE III - 16 SUPERIMPOSED EXPERIMENTAL AND SIMULATED ESR SPECTRA

in this study. The relative sizes and shapes of these structures strongly suggest the presence of phenyl-type free radicals. It is evident that other radical species are also present.

CHAPTER IV

COMPUTER PROGRAMS FOR SPECTRAL ANALYSIS

A. THE MAIN PROGRAM FOR SPECTRAL ANALYSIS

The main program consists of twelve major subroutines. Figure IV-1 is a flowchart of the main program. The main program opens two disk files for the storage and retrieval of ESR spectra. In one of the files, experimental ESR spectra were previously stored for analysis.

According to the operational codes supplied to it via the CRT terminal, the program branches to different subroutines or to one of the linkage programs to perform special functions in spectral analysis. The main program establishes an array and passes it to various subroutines as parameter. The array contains a ESR spectrum to be analyzed. This same array is shared with other linkage programs by means of blank COMMON.

Upon completion of a particular function via a sub-routine or linkage program, the main program is ready to receive a new operation code for further analysis procedures. An operation code larger than the total number of major subroutines and linkage programs, sixteen in this case, terminates the entire program. The main program is stored on the disk under the name PLSPEC.

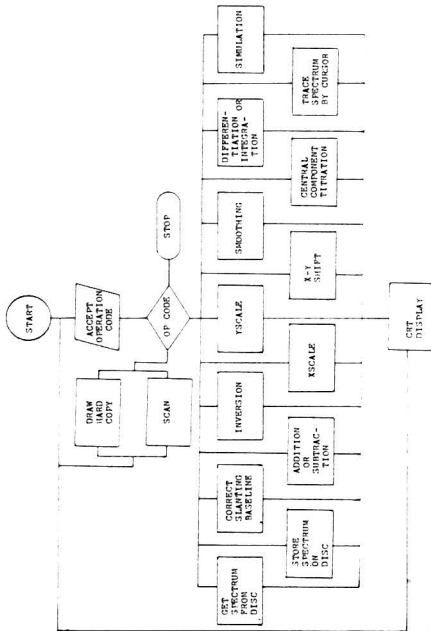


FIGURE IV - 1 FLOWCHART FOR MAIN PROGRAM PLSPEC

B. MAJOR SUBROUTINES:

Twelve major subroutines, some of which have their own subroutines, were written. Each performs a special function in the process of spectral analysis.

The following is a description of the subroutines. F is the array which contains a spectrum to be analyzed. It is passed to different subroutines as a parameter.

1. Subroutines ESRDIS (F)

This subroutine retrieves a particular ESR spectrum from the disk after accepting the required file number and records number via the terminal.

2. Subroutine ESRSTR (F)

A spectrum stored in an array F may be transferred to disk by specifying disk locations from the terminal.

3. Subroutine ESRSLP (F)

A systematic drift in the baseline during the recording of a spectrum frequently occurs. This subroutine subtracts a slanting portion from the spectrum to restore a horizontal baseline. Coordinates of two points on the slanting spectrum are entered via the terminal. The slope of the line joining the two points is calculated and a resulting ramp function is subtracted from the original slanting spectrum restoring a horizontal baseline. Values of the two coordinates were determined by the linkage program, ESRTRA, described in the latter part of this chapter.

Figures IV-2 & 3 show a slanting spectrum before and after restoring to a horizontal baseline.

4. Subroutine ERSUM (F)

Often the addition or subtraction of certain components to or from a complex spectrum helps to clarify the structure of a spectrum. The subroutine ERSUM calls from disk two spectra according to file and records numbers supplied to it via the terminal. A signed integer serves as a code to add or subtract the two spectra. Figures IV-4 to 7 show two spectra and their sum and difference spectra.

5. Subroutine ESRINV (F)

Experimental conditions sometimes give ESR spectra that are 180 degrees out of phase with other spectra. Subroutine ESRINV serves to invert a spectrum about its average ordinate value. Figure IV-8 shows the inversion of Figure IV-4.

6. Subroutine XSCALE (F)

To compare ESR spectra recorded with different coordinate scales or to compare a simulated spectrum with an experimental one, it is necessary to be able to rescale one or both spectra in the x direction. This subroutine accepts a multiplication factor and then modifies the spectrum accordingly. A value greater than one means expansion while a value less than one means contraction. All features expanded outside the range of the original array are lost. Therefore, shifting may be necessary before

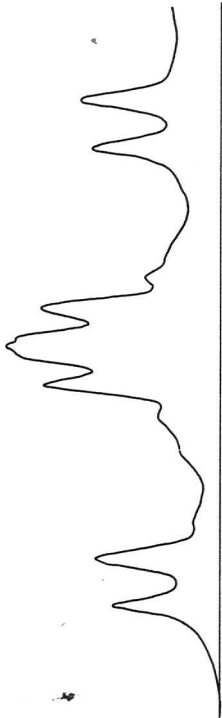


FIGURE IV - 2 INTEGRATED ESR SPECTRUM WITH SLANTING BASELINE

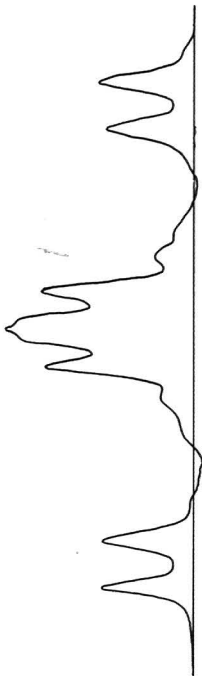


FIGURE IV - 3 ESR SPECTRUM WITH SLANTING BASELINE CORRECTION

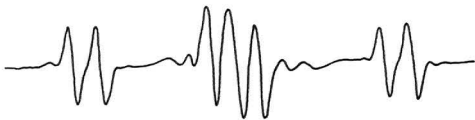


FIGURE IV - 4 A SAMPLE ESR SPECTRUM, A.



FIGURE IV - 5 A SAMPLE ESR SPECTRUM, B.



FIGURE IV - 6 SUMMATION SPECTRUM, A + B.



FIGURE IV - 7 DIFFERENCE SPECTRUM, A - B.



FIGURE IV - B INVERSION OF THE SPECTRUM OF FIGURE IV - 4.

expansion to preserve needed portion of the spectrum. Figures IV-9 and IV-10 show the contracted and expanded spectra of the one shown in Figure IV-4.

7. Subroutine ESRSHF (F)

In order to achieve alignment of spectra before addition or subtraction, it is necessary to shift a spectrum along the X-axis. Subroutine ESRSHF shift a spectrum left or right according to the value supplied to it via the terminal. A positive integer signifies shift right while a negative integer signifies shift left. Values shifted out of the array range are lost.

8. Subroutine YSCALE (F)

Subroutine YSCALE multiplies the Y values of a spectrum by a multiple entered via the terminal.

9. Subroutine ESRSMO (F)

A convolution procedure (23) of an eleven point quadratic least-square curve fitting is used to smooth a spectrum.

10. Subroutine ESRCPY

This subroutine supplies a hard copy of what is being displayed on the graphic terminal via a Calcomp plotter.

11. Subroutine SCOPX (F)

Upon completion of various subroutines or the execution of linkage programs, subroutine SCOPX is called to display the resultant spectrum.

12. Subroutine CNTLTL

For the analysis of spectra of gamma-irradiated single

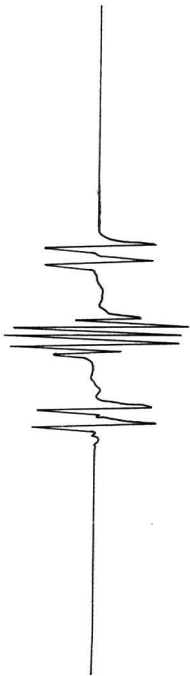


FIGURE IV - 9 HORIZONTAL CONTRACTION OF SPECTRUM OF FIGURE IV - 4 TO $1/3$ ITS ORIGINAL SPAN

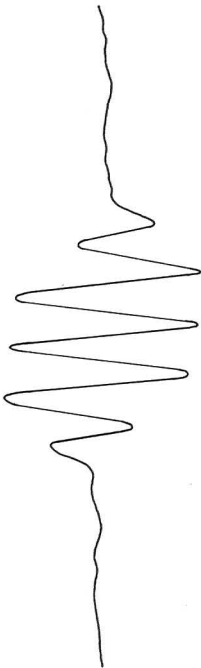


FIGURE IV - 10 HORIZONTAL EXPANSION OF SPECTRUM OF FIGURE IV - 4 BY 3 TIMES

crystals of 1,2,3-benzene tricarboxylic acid dihydrate, it is necessary to titrate central components of each spectrum with components from both wings. Wing structures from both high field and low field positions are shifted to the center to coincide with corresponding features and subtracted from the spectrum. The resultant spectrum is displayed for analysis. See Figure 11.

C. LINKAGE PROGRAMS:

Because of computer memory restrictions, four independent programs are linked to PLSPEC to facilitate the total function of spectral analysis. Each program is separately loaded on the disk with a different program name. Linkage of programs is made by the Call Link function.

1. ESRSCN

Subroutine ESRSCN provides a sequential display of all ESR spectra stored on the disk. It opens the disk file in which spectra are stored and displays each spectrum in sequence with a sequence number. The setting of computer console sense switches is used to stop the scan at any desired point and the scan may continue or be terminated by an operation code entered via the terminal.

2. ESRTRA

To obtain pertinent information from a spectrum, such as line width or location, a cursor is used to trace along a spectrum. When the cursor arrives at a particular point of interest, the setting of a sense switch stops



A. ORIGINAL SPECTRUM



B. COMPONENTS TO BE SUBTRACTED



C. RESULTANT SPECTRUM

FIGURE IV-11 TITRATION OF CENTRAL COMPONENTS

the trace. The X, Y-coordinates of the stopping point of the cursor are displayed. The trace continues with the resetting of the sense switch. Figure IV - 12 shows the cursor and the display of its coordinates.

3. ESRDIX

This program numerically differentiates or integrates a given spectrum. An eleven point convolution method (23) is used. Higher degrees of differentiation and integration are allowed. A positive integer code indicates the degree of differentiation while a negative integer denotes the degrees of integration. The resultant spectrum is normalized to full Y-scale before displaying at the graphic terminal. Figures IV - 13 & 14 show the integrated and differentiated spectrum of Figure IV - 4.

4. PLESR

a. The Main Program

The main program accepts appropriate spectral parameters and calls the subroutine, ESR, for the simulation of ESR spectra.

b. Subroutine ESR

This subroutine accepts the number of groups of equivalent nuclei for a particular free radical, the spin quantum number for each group, and the hyperfine splitting constants of each group. It calls subroutine PLBNXP to calculate the number of lines and their relative intensities, HS (I) & DS (I). Subroutine

470.00

200.32

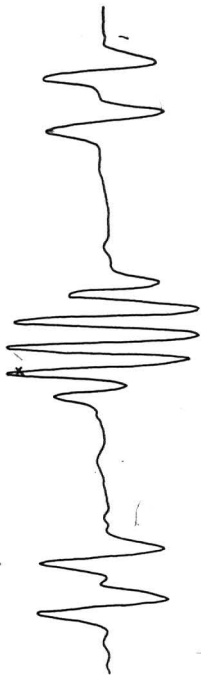


FIGURE IV-12 ESR SPECTRUM WITH CURSOR AND ITS COORDINATES DISPLAYED

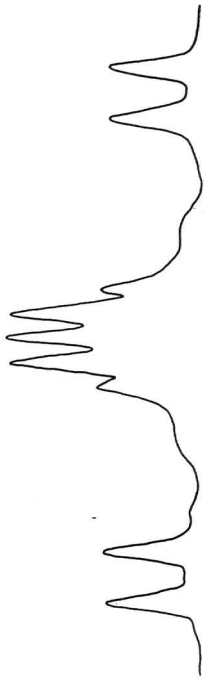


FIGURE IV-13 INTEGRATED ESR SPECTRUM OF FIGURE IV-4.

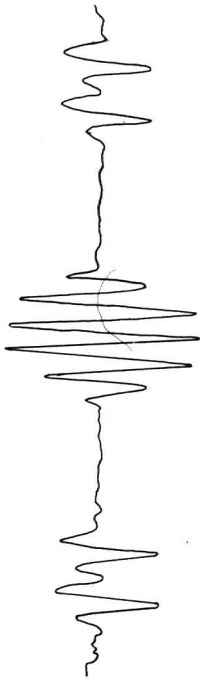


FIGURE IV-14 DIFFERENTIATED ESR SPECTRUM OF FIGURE IV-4.

PLBNXP accepts nuclei of any integral or half integral quantum numbers.

After normalizing DS (I) to the scale of the defined display ordinate, line spectra are displayed by calling subroutine PLINE.

c. Subroutine ESRSPC

The subroutine ESRSPC generates and displays the spectra in the form specified by operation codes passed to it from the main program. Figures IV - 15 to 18 are some sample displays of PLESR.



FIGURE IV - 15 SIMULATED GAUSSIAN ABSORPTION ESR SPECTRUM OF A PROTON INTERACTING WITH 3 EQUIVALENT SPIN $3/2$ NUCLEI

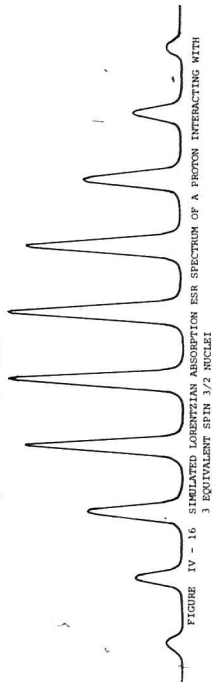


FIGURE IV - 16 SIMULATED LORENTZIAN ABSORPTION ESR SPECTRUM OF A PROTON INTERACTING WITH 3 EQUIVALENT SPIN $3/2$ NUCLEI

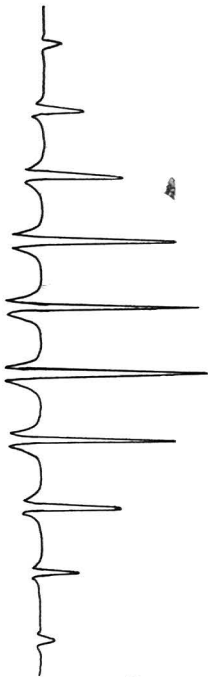


FIGURE IV-17 SECOND DERIVATIVE OF SPECTRUM IN FIGURE 16

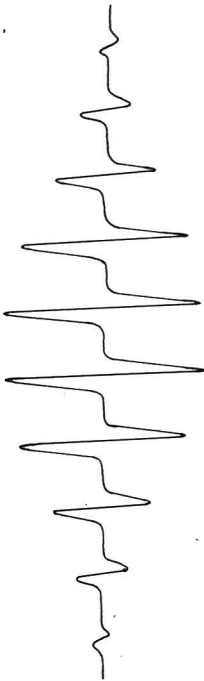


FIGURE IV-18 FIRST DERIVATIVE OF SPECTRUM IN FIGURE 16

CHAPTER V

SUMMARY AND CONCLUSIONS

A. FREE RADICALS IN GAMMA-IRRADIATED HEMIMELLITIC ACID DIHYDRATE SINGLE CRYSTAL :

Gamma irradiation at room temperature produced several radical species. Of these the cyclohexadienyl-type free radical was identified. It was formed by hydrogen addition at the C₄ or C₆ positions predominantly. Principal hyperfine coupling constants were determined. The isotropic hyperfine interaction constants were found to be 7.86 gauss and 45.99 gauss, respectively, for the alpha proton and the methylene protons. They agree well with published results of these free radicals in aqueous solutions. Power saturation studies and computer-assisted central components titration reveal the presence of other free radicals. Phenyl - type radicals were highly probable.

Further investigations should be made to correlate the crystal axes to the unit cell orientation. The degree of agreement between the direction cosines of the normal to the plane of the benzene rings and the direction of the intermediate principal hyperfine coupling constant, provides information on the geometrical changes of the molecule due to gamma irradiation.

Synthesis of selectively deuterated molecules would help to identify different free radicals. The source of the adduct hydrogen atom may be ascertained. Thus the hydrogen addition process may be clarified.

Jen, Foner, Cochran, and Bower (24) found that in solid matrix, deuterium atoms gave an overall triplet splitting approximately $1/3.27$ of that of protons. Therefore it is possible to simulate spectra of selectively deuterated cyclohexadienyl-type free radicals. This is done by changing the appropriate quantum number from $1/2$ to 1 and reducing the associated hyperfine coupling constant by a factor of $1/6.54$ during simulation. Figures V - 1 (b) to (k) are simulated spectra of selectively deuterated cyclohexadienyl-type radicals. They are modifications of the spectrum shown in Figure V - 1(a). In Figure V - 1(b), the C_5 proton replaced by a deuterium atom. Figure V - 1(c) shows the effects of replacement of one methylene proton and the C_5 proton by deuterium atoms. In Figure V - 1(d), the other methylene proton, which has a slightly greater isotropic hyperfine coupling constant, and the C_5 proton are replaced. Figure V - 1(e) is a summation of the spectra in Figures V - 1(c) and V - 1(d).

If the spectrum of cyclohexadienyl-type free radicals from 5-monodeuterohemimellitic acid dihydrate crystal shows close similarity with the spectrum in Figure V - 1(b), one may exclude the possibility of the adduct hydrogen atom coming from the C_5 proton of another molecule. On the other hand, if the experimental spectrum shows close similarity with either Figure G - 1(c) or V - 1(d), it may be concluded that the source of the adduct hydrogen comes from the C_5 proton of another molecule, and the addition is stereospecific. If addition is non-stereospecific, a composite spectrum which is the sum of the spectra in Figures V - 1(c) and V - 1(d) will result. See Figure V - 1(e). Partial stereospecificity

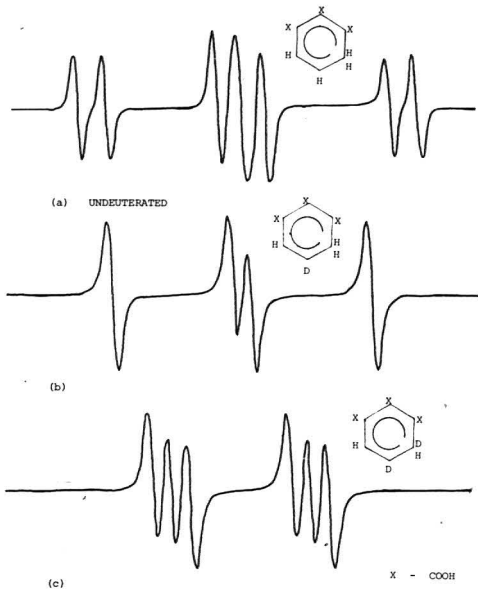
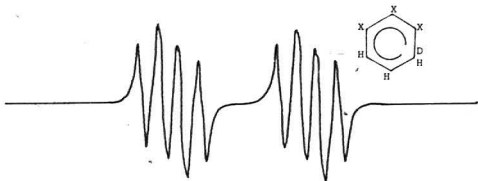
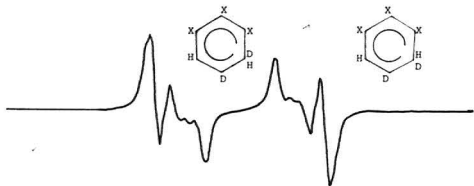
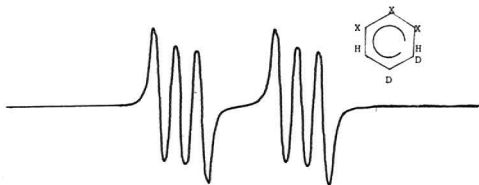
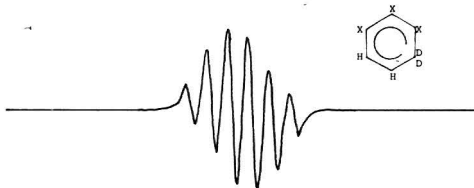
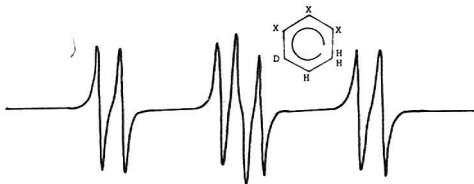
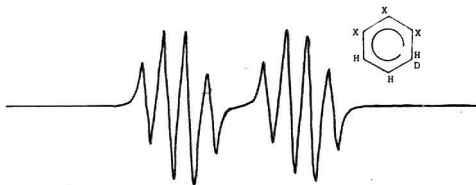


FIGURE V - 1 ESR SPECTRA OF CYCLOHEXADIENYL-TYPE FREE RADICALS DERIVED FROM GAMMA-IRRADIATED HEMIMELLITIC ACID OR MONODEUTEROHEMIMELLITIC ACID SINGLE CRYSTALS AT AN ARBITRARY ORIENTATION (SIMULATIONS)



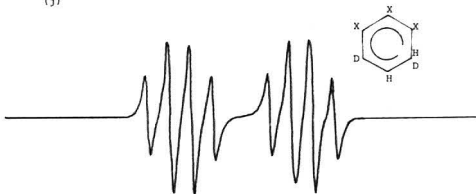
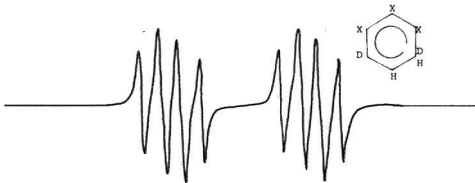
X - COOH

FIGURE V - 1 CONT.



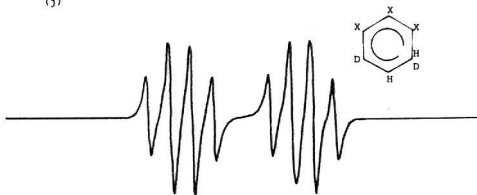
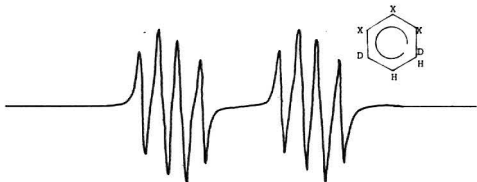
X - LOOH

FIGURE V - 1 CONT.



X - COOH

FIGURE V - 1 ~~cont.~~



X - COOH

FIGURE V - 1 cont.

can be evaluated by adding the same two spectra in varying proportions. A similar analysis can be carried out for cyclohexadienyl-type free radicals in gamma-irradiated 4- or 6- monodeuterohemimellitic acid single crystals. An experimental spectrum that is similar to one of those shown in Figure V - 1(f), (g), (h) or similar to a composite mix of any combination of the three precludes the possibility of adduct hydrogens coming from the 4 or 6 positions. If adduct hydrogens were abstracted from the 4 or 6 positions, spectrum similar to any one or any combination of those in Figures V - 1(i), (j), (k), would be expected. Thus the source of the adduct hydrogens can be deduced. The process of the formation of the cyclohexadienyl-type free radicals may be ascertained.

B. COMPUTER-ASSISTED ESR SPECTRAL ANALYSIS

In the analysis of gamma-irradiated single crystals of 1,2,3-benzene tricarboxylic acid dihydrate, the necessity of the use of the digital computer is evident. Several programs written in FORTRAN IV are developed for this study. With proper modifications they are adaptable to many areas of research that requires spectral analysis.

Operating in an interactive mode, the computer with its graphics and keyboard terminals enables the investigator to carry out different analysis procedures by entering appropriate operation codes and necessary parameters. Many of these procedures would be too tedious to be practical or too imprecise without the use of a computer.

After a spectrum is called from a disc and displayed at the CRT terminal, inversion is carried out if it is 180° out of phase. An eleven-point moving quadratic least-square curve fitting is done when data smooth-

ing is required. Pertinent coordinates are obtained with a cursor, which traces along the experimental curve. Differentiation helps to ascertain the field values of different absorption lines. Integration makes it possible to compare relative line intensities. It can also be used to assess the population of unpaired electrons.

A horizontal base line is restored for a slanting spectrum. Addition or subtraction of two or more curves clarifies superimposed spectral lines. Central titration of a cyclohexadienyl-type free radicals spectrum is done by shifting the high and low field structures by measured amounts to the central components and then subtracting amounts from the components. This clarifies the composition of the central components.

Spectral simulations based on measured hyperfine coupling constants assure proper interpretation of the hyperfine splittings. Spectra constructed with theoretical coupling constants have predictive value, waiting for experimental confirmation. They may also help to clarify certain unidentified features on an experimental curve.

No claim is made that the programs or the analysis procedures are done in the most efficient manner. Continuous development and refinement are required to meet the need of future investigators.

For ESR studies, it is desirable to write programs that provide computer curve fitting. More precise experimental parameters may be obtained. Polycrystalline spectrum simulation from principal interaction constants can help to show the composite mix of the spectrum.

For general spectral analysis, automated computation of the absorption line peak and intensity is desirable. Smoothing that allows the user to select the number of points as well as the degree of the fitting polynomial should be useful. A general curve-fitting program that accepts users' specifications of function and variables should have broad applications.

REFERENCES

1. J.R. Morton, Electron Spin Resonance Spectra of Oriented Free Radicals, Chem. Rev., 64, 453. 1964.
 2. Charles P. Poole, Jr., and Horacio A. Farach, The Theory of Magnetic Resonance, Wiley Interscience, John Wiley & Son Inc., N.Y., 1972.
 3. Jean C. Kertesz, Michael B. Wolf, and Walter Wolf, Comp. Prog. in Biomed., 4, 21, 1974.
 4. Charles Klopfenstein, Patricia Jost, and O. Hayes Griffith, Computers in Chemical and Biochemical Research, Klopfenstein and Wilkins, Ed., Academic Press, N.Y., 1972.
 5. L.C. Allen, H.M. Gladney, and S.H. Glarum, Resolution Enhancement of Spectra of Chemical and Physical Interest. J. Chem. Phys., 40, 3135-3141, 1974.
 6. A. Bauder and R.J. Rollie, J. Molec. Spectrosc. 27, 110-116, 1968.
 7. D.W. Posener, J. Magn. Resonance, 14, 129-140, 1974.
 8. H.M. Gladney, IBM Research Report RJ-318, October 16, 1964.
 9. D.K. Ghosh, D.H. Whiffen, Molec. Phys., 2, 285-300, 1959.
 10. H.M. McConnell and T. Strathdee, Molec. Phys. 2, 129-138, 1959.
 11. C.P. Slichter, Principles of Magnetic Resonance, Harper and Ros, N.Y., 1963.
 12. S.J. Wyard (Editor), Solid States Biophysics, McGraw-Hill Book Company, N.Y., 1969.
 13. John E. Wertz and James R. Bolton, Electron Spin Resonance, Elementary Theory and Practical Applications, McGraw-Hill, N.Y., 1972.
 14. N.M. Atherton, Electron Spin Resonance Theory and Applications, Halsted Press, John Wiley & Sons Inc., N.Y., 1973.
 15. C.P. Poole, Jr., Electron Spin Resonance: A comprehensive Treatise on Experimental Techniques, Interscience Publishers, a division of John Wiley & Sons, N.Y., 1967.
- 

16. Shun-Ichi Ohnishi, Tadayoshi Tanei, and Isamu Nitta, *J. Chem. Phys.*, 37, 2402, 1962.
17. R. W. Fessenden and R.H. Schuler, *J. Chem. Phys.*, 39, 2147, 1963.
18. Paul H. Kasai, E. Hedaya, and Earl B. Whipple, *J. Am. Chem. Soc.*, 91, 4364, 1969.
19. D. Campbell and D.T. Turner, *Canad. J. Chem.*, 45, 1967.
20. Klaus Eiben and Robert H. Schuler, *J. Chem. Phys.*, 62, 8, 3093 - 3108, 1975.
21. F. Mo and E. Adman, *Acta Cryst.*, B 31(1), 192-198, 1975.
22. A Carrington and Andrew D. McLachlan, *Introduction to Magnetic Resonance*, Harper and Row, N.Y., 1967.
23. A Savitzky and M.J.E. Golay, *Anal. Chem.*, 36, 8, 1628-1635, 1964.
24. C.K. Jen, S.N. Foner, E.L. Cochran, and V.A. Bowers, *Phys. Rev.*, 104, 846, 1956.

Abstract

COMPUTER ASSISTED ELECTRON SPIN RESONANCE
SPECTRAL ANALYSIS OF TRAPPED RADICALS

by Philip M. W. Law

A set of general purpose FORTRAN IV programs have been written during this study to assist in the analysis of complex spectra. An interactive approach is adopted, utilizing the computer and graphics terminals of the Scientific Computation Facility at Loma Linda University. Some procedures carried out are inversion, coordinates scaling, smoothing, differentiation and integration, correction for slanting baseline, addition and subtraction, and spectral simulation.

As an application, the programs are used to assist in the study of free radicals in gamma-irradiated single crystals of 1,2,3-benzene tricarboxylic acid dihydrate by electron spin resonance spectroscopy. It is found that the predominant free radical formed by gamma-irradiation of the acid crystals at room temperature, is a cyclohexadienyl-type free radical formed by the addition of a hydrogen at the C₄ or C₆ position. Principal hyperfine coupling constants are -11.58 MHz, -20.79 MHz, and -33.92 MHz for the C₅ proton. Isotropic hyperfine coupling constants are found to be -22.10 MHz for the C₅ proton, and 119.96 MHz and 137.54 MHz for the two methylene protons.